PLOS | ONE

RESEARCH ARTICLE

Mutation in *LIM2* Is Responsible for Autosomal Recessive Congenital Cataracts

Bushra Irum[1,2], Shahid Y. Khan[1], Muhammad Ali[1], Haiba Kaul[1], Firoz Kabir[1], Bushra Rauf[1,2], Fareeha Fatima[2], Raheela Nadeem[2], Arif O. Khan[3], Saif Al Obaisi[3], Muhammad Asif Naeem[2], Idrees A. Nasir[2], Shaheen N. Khan[2], Tayyab Husnain[2], Sheikh Riazuddin[2,4,5], Javed Akram[4,5], Allen O. Eghrari[1], S. Amer Riazuddin[1,6]*

1 The Wilmer Eye Institute, Johns Hopkins University School of Medicine, Baltimore, MD, 21287, United States of America, **2** National Centre of Excellence in Molecular Biology, University of the Punjab, Lahore, 53700, Pakistan, **3** King Khaled Eye Specialist Hospital, Riyadh, 12329, Saudi Arabia, **4** Allama Iqbal Medical College, University of Health Sciences, Lahore, 54550, Pakistan, **5** National Centre for Genetic Diseases, Shaheed Zulfiqar Ali Bhutto Medical University, Islamabad, 44000, Pakistan, **6** McKusick-Nathans Institute of Genetic Medicine, Johns Hopkins University School of Medicine, Baltimore, MD, 21205, United States of America

* riazuddin@jhmi.edu

CrossMark
click for updates

OPEN ACCESS

Citation: Irum B, Khan SY, Ali M, Kaul H, Kabir F, Rauf B, et al. (2016) Mutation in *LIM2* Is Responsible for Autosomal Recessive Congenital Cataracts. PLoS ONE 11(11): e0162620. doi:10.1371/journal.pone.0162620

Editor: Yong-Bin Yan, Tsinghua University School of Life Sciences, CHINA

Received: April 4, 2016

Accepted: August 25, 2016

Published: November 4, 2016

Copyright: This is an open access article, free of all copyright, and may be freely reproduced, distributed, transmitted, modified, built upon, or otherwise used by anyone for any lawful purpose. The work is made available under the Creative Commons CC0 public domain dedication.

Data Availability Statement: The minimal dataset needed for replication can be found and accessed within the paper.

Funding: This study was supported in part by the National Eye Institute, grant R01EY022714 (SAR), the Knights Templar Eye Foundation grant (SAR), King Khaled Eye Specialist Hospital-Johns Hopkins University collaboration grant (SAR), the National Academy of Sciences, Washington DC USA, and the Higher Education Commission, Islamabad Pakistan.

Abstract

Purpose

To identify the molecular basis of non-syndromic autosomal recessive congenital cataracts (arCC) in a consanguineous family.

Methods

All family members participating in the study received a comprehensive ophthalmic examination to determine their ocular phenotype and contributed a blood sample, from which genomic DNA was extracted. Available medical records and interviews with the family were used to compile the medical history of the family. The symptomatic history of the individuals exhibiting cataracts was confirmed by slit-lamp biomicroscopy. A genome-wide linkage analysis was performed to localize the disease interval. The candidate gene, *LIM2* (lens intrinsic membrane protein 2), was sequenced bi-directionally to identify the disease-causing mutation. The physical changes caused by the mutation were analyzed *in silico* through homology modeling, mutation and bioinformatic algorithms, and evolutionary conservation databases. The physiological importance of LIM2 to ocular development was assessed *in vivo* by real-time expression analysis of *Lim2* in a mouse model.

Results

Ophthalmic examination confirmed the diagnosis of nuclear cataracts in the affected members of the family; the inheritance pattern and cataract development in early infancy indicated arCC. Genome-wide linkage analysis localized the critical interval to chromosome 19q with a two-point logarithm of odds (LOD) score of 3.25. Bidirectional sequencing identified a novel missense mutation, c.233G>A (p.G78D) in *LIM2*. This mutation segregated

Competing Interests: The authors have declared that no competing interests exist.

with the disease phenotype and was absent in 192 ethnically matched control chromosomes. *In silico* analysis predicted lower hydropathicity and hydrophobicity but higher polarity of the mutant *LIM2*-encoded protein (MP19) compared to the wild-type. Moreover, these analyses predicted that the mutation would disrupt the secondary structure of a transmembrane domain of MP19. The expression of *Lim2*, which was detected in the mouse lens as early as embryonic day 15 (E15) increased after birth to a level that was sustained through the postnatal time points.

Conclusion

A novel missense mutation in *LIM2* is responsible for autosomal recessive congenital cataracts.

Introduction

Cataracts are opacifications that occur in the ocular lens, and are the leading cause of vision loss in children globally [1,2]. Cataracts can be morphologically diverse and classification systems are frequently based on the location of opacity. Congenital cataracts can be divided by these traits: total (mature or complete), polar (anterior or posterior), zonular (nuclear, lamellar, or sutural), and capsular or membranous [3].

Congenital cataracts are also genetically heterogeneous, and can manifest as an autosomal dominant or recessive trait. Autosomal recessive congenital cataracts (arCC) have been associated with loci and genes on chromosomes 1p, 1q, 3p, 3q, 6p, 7q, 8p, 9q, 11q, 16q, 17q, 19q, 20p, 21q, and 22q [4–20]. Pathogenic mutations have been reported in EPH receptor A2 (*EPHA2)*, connexin50 (*GJA8)*, FYVE and coiled-coil domain containing 1 (*FYCO1*), glucosaminyl (N-acetyl) transferase 2 (*GCNT2)*, acylglycerol kinase (*AGK*), tudor domain containing 7 (*TDRD7*), crystallin alpha B (*CRYAB*), heat shock transcription factor 4 (*HSF4*), galactokinase 1 (*GALK1*), lens intrinsic membrane protein 2 (*LIM2*), beaded filament structural protein 1 (*BFSP1*), crystallin alpha A (*CRYAA*), lanosterol synthase (*LSS*), crystallin beta B1 (*CRYBB1*), and crystallin beta B3 (*CRYBB3*) [5,6,9,13–15,17–25].

The product of *LIM2* is a 173-amino-acid membrane protein, named MP19, with four transmembrane domains [26]. MP19 is the second most abundant integral membrane protein present in the ocular lens fiber cells of vertebrates [27,28]. It localizes to junction regions of the lens fiber cell membrane as well as throughout the fiber cell membrane, suggesting a role in junction communication [29,30].

To date, only two missense mutations in *LIM2* have been associated with autosomal recessive cataracts. Pras and colleagues reported the c.313T>G (p.F105V) mutation in a family with presenile cortical cataracts and Ponnam and colleagues reported the c.587G>A (p.G154E) mutation in a family with arCC [17,31]. Here, we report a novel missense mutation in *LIM2* in a consanguineous Pakistani family with arCC. This is the first causal mutation for arCC reported in the Pakistani population.

Materials and Methods

Patient Recruitment and Clinical Evaluation

A total of 300 plus consanguineous Pakistani families with non-syndromic cataracts were invited to participate in a collaborative study to understand the genetic aspects of arCC.

Institutional Review Board (IRB) approval was obtained from the National Eye Institute (Bethesda, MD), Johns Hopkins University School of Medicine (Baltimore, MD), and the National Centre of Excellence in Molecular Biology (Lahore, Pakistan). All participating subjects gave informed written consent consistent with the tenets of the Declaration of Helsinki.

A detailed medical history was obtained by interviewing family members. Ophthalmic examinations, including slit-lamp microscopy, were performed at the Layton Rahmatulla Benevolent Trust (LRBT) Hospital (Lahore, Pakistan). Approximately 10 ml of blood was drawn from all participating members and the samples were stored in 50 ml Sterilin Falcon tubes with 20 mM EDTA. Genomic DNA was extracted as previously described [32,33].

Genome-Wide Scan

Applied Biosystems MD10 linkage mapping panels (Applied Biosystems, Foster City, CA) were used to complete a genome-wide scan for the family, designated PKCC214. Multiplex polymerase chain reaction (PCR) was completed as previously described [32,33]. PCR products were mixed with a loading cocktail containing 400HD size standards and resolved in a 3100 Genetic Analyzer (Applied Biosystems). Genotypes were assigned using GeneMapper software from Applied Biosystems.

Linkage Analysis

Two-point linkage analysis was performed using the FASTLINK version of MLINK from the LINKAGE Program Package (provided in the public domain by the Human Genome Mapping Project Resources Centre, Cambridge, UK) [34,35]. Maximum LOD scores were calculated using PLINK (Shaun Purcell, Boston, MA). arCC was analyzed as a fully penetrant trait with an affected allele frequency of 0.001. The marker order and distances between the markers were obtained from the NCBI (National Center for Biotechnology Information, Bethesda, MD) chromosome 19 sequence maps.

Sanger Sequencing

Primer pairs for individual exons were designed using the Primer3 program. The primer sequences and amplification conditions are provided in Table 1. The PCR amplifications were performed in 10 μl reactions with 20 ng of genomic DNA. The PCR primers for each exon were used for bidirectional sequencing with the BigDye Terminator Ready Reaction mix, according to the manufacturer's instructions (Thermo Fisher Scientific, Waltham, MA). Sequencing products were dissolved in 10 μl of Formamide (Applied Biosystems) and resolved on an ABI PRISM 3100 Genetic Analyzer (Applied Biosystems). Sequencing results were assembled with ABI PRISM sequencing analysis software, version 3.7, and analyzed with SeqScape software (Applied Biosystems).

Table 1. Primer sequences used for the amplification of *LIM2* coding exons.

Exon	Forward	Reverse	Annealing Temperature (˚C)
1	GACCATTGTGTAGGGAGGCTTA	GCTTCCTGAGTCCTAGGTGAGA	68
2	CGTCTAGGTCTCCATCTCCTTC	CCCAACTTAACCTTCAAACCAG	68
3	TTTCATCTCAGAGGTAGCAGCA	AGGAGTAAGGGGTGAGAATGGT	68
4	ACCCCTTTCCCCAATCTTAGTT	ACTCCATAGGCCTGGAGTCTTC	68
5	GGATACCCAGGGAGAAAGAGAGT	ACGGGGACTTGAGTCTTCTCAG	68

doi:10.1371/journal.pone.0162620.t001

Prediction Analysis

The possible impact of an amino acid substitution on the structure of MP19 at the location of the missense mutation was examined with Condel (http://bg.upf.edu/fannsdb), SIFT (http://sift.jcvi.org), PolyPhen-2 (http://genetics.bwh.harvard.edu/pph), Mutation Assessor (http://mutationassessor.org), and FATHMM (http://fathmm.biocompute.org.uk). Evolutionary conservation of the mutated amino acid in MP19 orthologs was examined using the UCSC Genome Browser (http://genome.ucsc.edu).

Biophysical Characteristics

The hydropathicity, optimized matching hydrophobicity, and polarity of the wild-type and mutant MP19 proteins were examined using ProtScale, a bioinformatics tool on the ExPASy Server (http://www.expasy.org/tools/protscale.html). Similarly, we used ProtScale to compute the isoelectric point (pI) of the wild-type and the mutant MP19 proteins.

Homology Modeling

Comparative homology modeling of MP19 was performed with predicted 3D structures, retrieved from ModBase, of the wild-type (P55344) and mutant MP19 sequences. The wild-type and mutated protein sequences were also loaded onto Swiss PDB viewer to produce homology models. Hydrogen bonding was incorporated into Swiss PDB Viewer, made available by the Swiss Institute of Bioinformatics (Geneva, Switzerland).

Real-Time Expression Analysis

The use of mice in this study was approved by the Johns Hopkins Animal Care and Use Committee (ACUC), and all experiments were performed in accordance with a protocol approved by the Johns Hopkins ACUC. Mouse (C57BL/6) lenses were obtained at different developmental stages, including embryonic day 15 (E15), day 18 (E18), at birth (P0), postnatal day 3 (P3), day 6 (P6), day 9 (P9), day 12 (P12), day 14 (P14), day 21 (P21), day 28 (P28), day 42 (P42), and day 56 (P56). Mice lenses were obtained as previously described [32,33]. Mice were exposed to CO_2 and, after cervical dislocation, the ocular lenses were isolated. Total RNA was isolated with TRIzol Reagent according to the manufacturer's instructions (Invitrogen, Carlsbad, CA). The quality and quantity of the total RNA were determined on a NanoDrop Lite Spectrophotometer (Thermo Fisher Scientific). First-strand cDNA synthesis was completed using the Superscript III kit according to the manufacturer's instructions (Invitrogen). Quantitative real-time PCR was performed on a StepOne Real-Time PCR System using commercially available TaqMan expression assays for *Lim2* and *Gapdh*, where the latter was used as an endogenous internal control (Applied Biosystems). The $2^{-\Delta CT}$ method was used to determine the relative expression, normalized to *Gapdh* expression, at each developmental stage.

Results

A consanguineous family, PKCC214, with four affected and three unaffected individuals (Fig 1) was recruited from the Punjab province of Pakistan. A detailed medical history was compiled from interviews with family members and available medical records, which showed that all affected individuals developed cataracts at birth (Table 2). The slit-lamp examinations confirmed the presence of cataracts in the affected individuals exhibiting bilateral nuclear cataracts (Fig 2).

We conducted genome-wide scans with the MD10 ABI PRISM panel set and calculated two-point LOD scores according to the method described in previous reports, with some

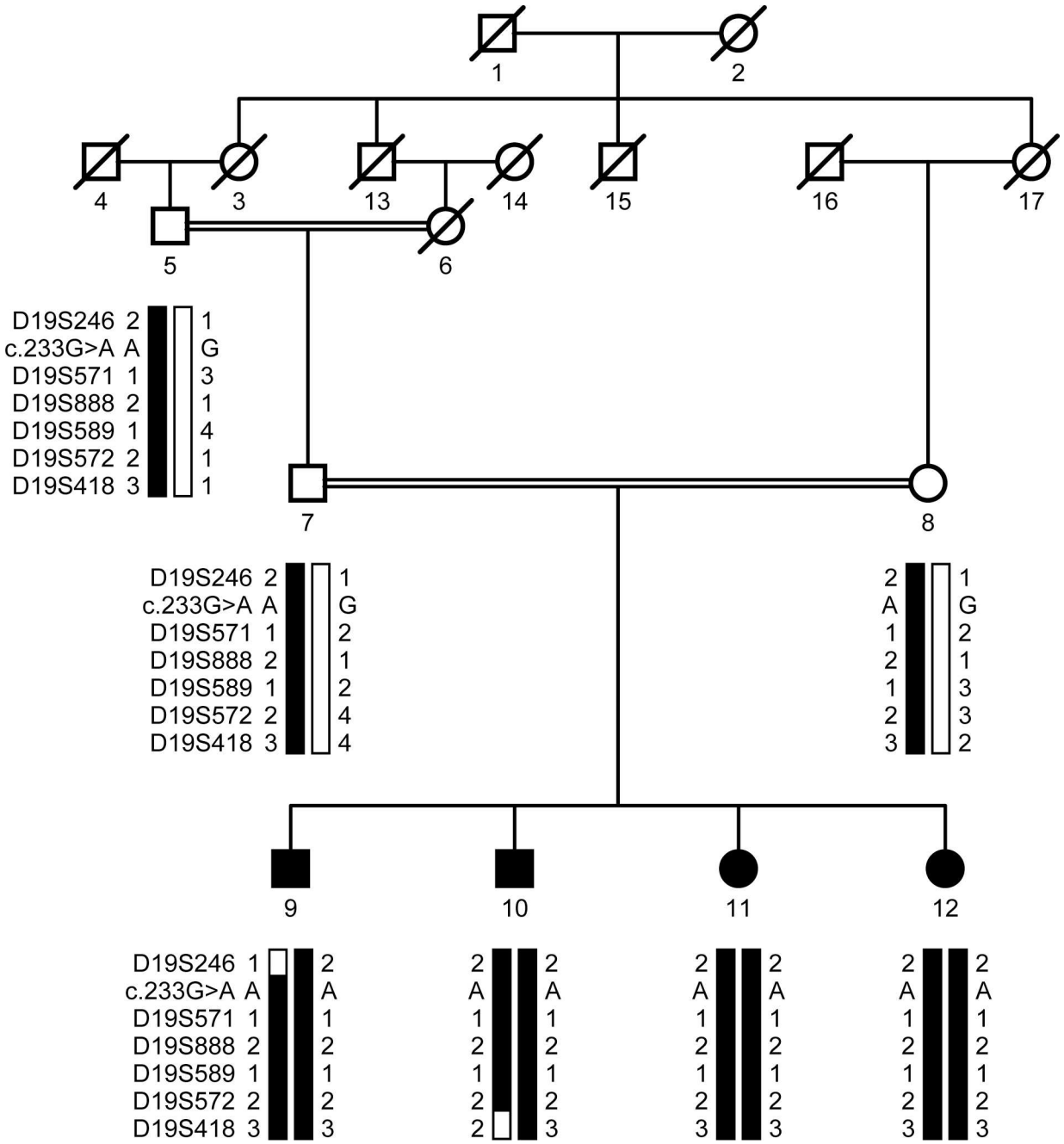

Fig 1. Pedigree drawing of the family PKCC214 with haplotypes of 6 adjacent chromosome 19q microsatellite markers. Alleles that constitute the risk haplotype are shaded black and alleles not co-segregating with cataracts are shown in white. Square: male; circle: female; filled symbol: affected individual; double line between symbols: consanguineous mating; diagonal line through symbol: deceased.

doi:10.1371/journal.pone.0162620.g001

modifications. Linkage was observed with chromosome 19q markers showing maximum LOD scores of 3.25, 3.25, 2.61, and 2.11 at $\theta = 0$ with D19S589, D19S572, D19S571, and D19S888, respectively (Table 3). Haplotype analysis confirmed that the genotypes of affected individuals of PKCC214 were homozygous for D19S571, D19S888, D19S589, and D19S572 while the unaffected individuals were heterozygous. Individual inspection of the haplotypes of PKCC214

Table 2. Clinical characteristics of individuals of PKCC214 who manifest symptoms of autosomal recessive congenital cataracts.

Individual ID	Gender	Age of onset	Age at Enrollment (years)	Visual Acuity (OD/OS)	Clinical Findings
9	M	birth	5	CF/CF	B/L nystagmus
10	M	birth	6	NA	NA
11	F	birth	4	CF/PL	B/L nystagmus; B/L pseudophakia
12	F	birth	8	NA	NA

Age of onset determined by the age at which the first symptoms manifested; CF: counting fingers; PL: perception of light; B/L: bilateral; NA: not available.

doi:10.1371/journal.pone.0162620.t002

supports the results of the linkage analysis and localizes the disease to a 14.5 cM interval between D19S246 and D19S418. A recombination event in affected individual 9 at D19S246 defines the proximal boundary while a recombination event in individual 10 at D19S418 sets

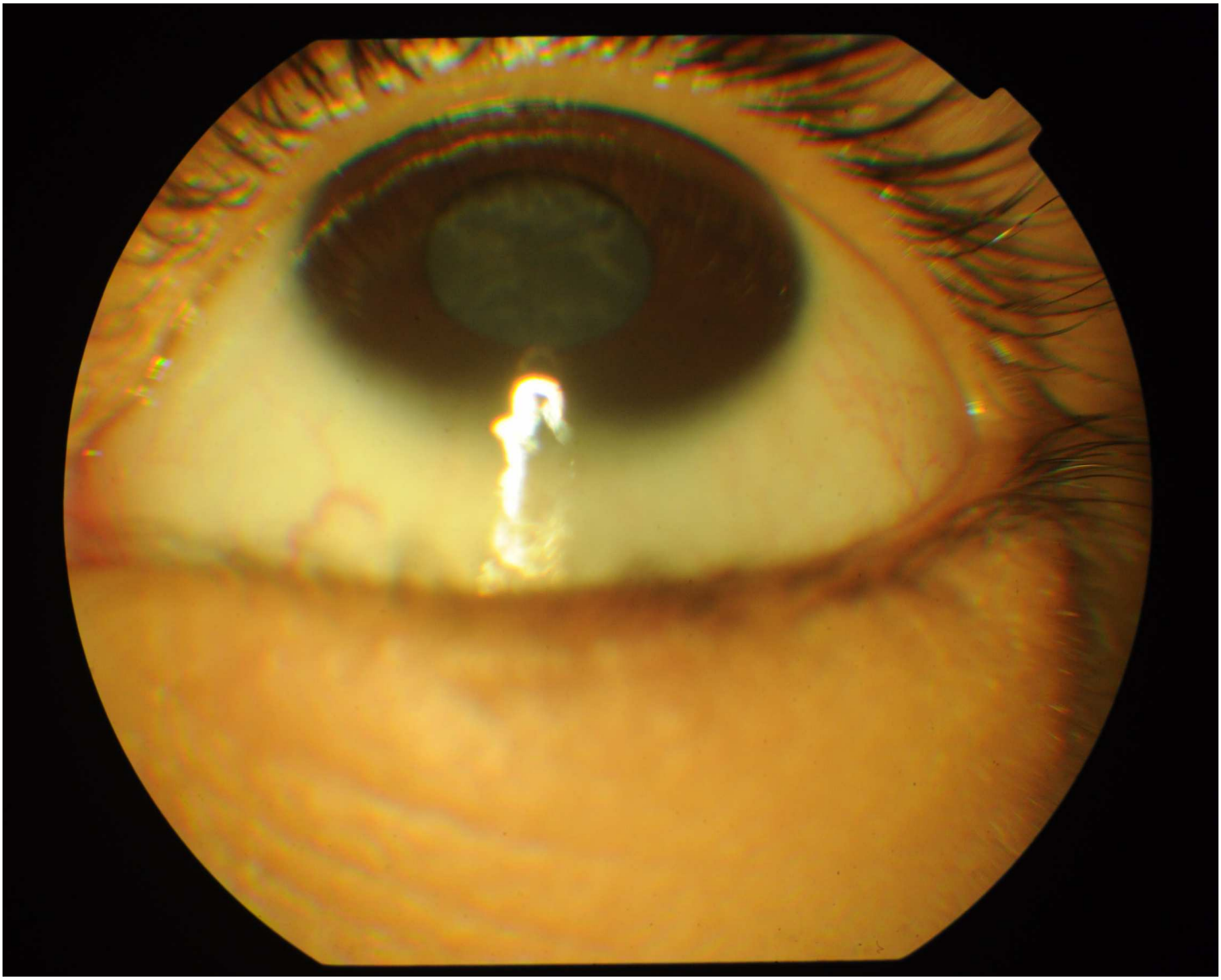

Fig 2. Slit-lamp photograph of affected individual 9 of PKCC214. This photograph depicts a nuclear cataract that developed during infancy.

doi:10.1371/journal.pone.0162620.g002

Table 3. Two-point LOD scores and microsatellite markers used for linkage analysis of PKCC214.

Marker	cM	Mb	0	0.01	0.05	0.09	0.1	0.2	0.3	Z_{max}	θ_{max}
D19S246	78.08	50.45	$-\infty$	0.07	0.60	0.69	0.69	0.58	0.35	0.69	0.09
D19S571*	84.08	52.79	2.61	2.56	2.36	2.15	2.10	1.57	1.04	2.61	0.0
D19S888*	85.87	53.15	2.11	2.06	1.87	1.67	1.63	1.14	0.64	2.11	0.0
D19S589	87.66	53.30	3.25	3.19	2.96	2.72	2.66	2.04	1.39	3.25	0.0
D19S572*	88.85	53.60	3.25	3.19	2.96	2.72	2.66	2.04	1.39	3.25	0.0
D19S418*	92.56	55.54	$-\infty$	0.66	1.17	1.23	1.22	1.04	0.73	1.23	0.09

An asterisk indicates markers from genome-wide scan.

doi:10.1371/journal.pone.0162620.t003

the distal boundary (Fig 1). We did not find a significant LOD score with any markers other than those of the region harboring the *LIM2* gene.

The linkage interval harbors more than 100 genes; however, only *LIM2* has previously been associated with cataractogenesis, according to the CatMap database. We sequenced the four coding exons, exon–intron boundaries, and the 5′ and 3′ UTR regions of *LIM2*. A novel missense mutation, c.233G>A, was identified in exon 3 that results in the substitution of aspartic acid for glycine at position 78 (Fig 3A and 3B). This variation segregated with the disease phenotype in PKCC214 and was not present in 192 ethnically matched control chromosomes. Moreover, this variant is not present in the 1000 Genomes database, the ExAC browser, the dbSNP database, or the Exome Variant Server. Importantly, glycine 78 and the amino acids in the immediate neighborhood are well-conserved in MP19 orthologs (Fig 3C). *In silico* analyses with the Condel, SIFT, PolyPhen-2, MutationAssessor, and FATHMM algorithms were all suggestive of the fact that the glycine substitution would not be tolerated and would be damaging to the native structure of the *LIM2*-encoded protein, MP19 (data not shown).

Next, we examined the impact of the c.233G>A mutation on the chemical characteristics of MP19. ProtScale software predicted that the mutant MP19 would have lower hydropathicity (Fig 4A and 4D) and lower hydrophobicity (Fig 4B and 4E) compared with the wild type protein. Moreover, the software predicted a higher polarity for mutant MP19 with respect to the wild type protein (Fig 4C and 4F). In parallel, we computed the isoelectric point (pI) of the mutant MP19. We found that the mutation lowers the isoelectric point of the mutant protein (pI: 9.94 vs. pI: 10.04 of the wild type MP19).

Computer modeling predicts MP19 to have four helical transmembrane domains, and two extracellular and three cytoplasmic topological domains (Fig 5A) [36]. To investigate the effect of the p.G78D mutation on the normal folding and protein conformation, we compared the ModBase-predicted 3D structures of the wild-type (P55344) and mutant MP19 (Fig 5B and 5C). The comparison suggests that the aspartic acid side chain of mutant MP19 forms bonds with the amino acids phenylalanine 10 (F10) and cysteine 74 (C74) (Fig 5C). The bond formation between the mutated amino acid, D78, and F10 of the first transmembrane domain is likely to disrupt the membrane-associated topology of the native protein structure.

As a first step in understanding the physiological significance of *LIM2* in the development of the ocular lens, we explored the expression of *Lim2* in our recently published mouse lens transcriptome. *Lim2* is expressed as early as embryonic day 15 [37]. Low levels of expression were observed in the embryonic stages; however, relatively higher expression was observed at the postnatal time points [37]. To further investigate the expression profile of *Lim2* in the mouse lens, we performed quantitative real-time PCR analysis at six additional postnatal time points and used the expression level at E15 as a reference for the comparison of the subsequent 11 time points. As shown in Fig 6, consistent with our previously published results, *Lim2* is

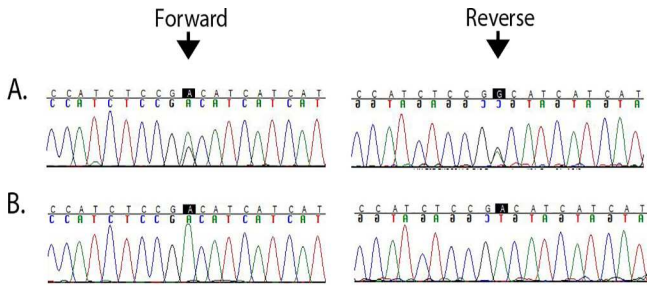

C.

Human	C_{74}	A_{75}	I_{76}	S_{77}	G_{78}	I_{79}	I_{80}	M_{81}	G_{82}
Chimp	C	A	I	S	G	I	I	M	G
Gorrila	C	A	I	S	G	I	I	M	G
Orangutan	C	A	T	S	G	I	I	M	G
Gibbon	C	A	T	S	G	I	I	M	G
Rhesus	C	A	T	S	G	I	I	M	G
Crab-eating macaque	C	A	T	S	G	I	I	M	G
Baboon	C	A	T	S	G	I	I	M	G
Green monkey	C	A	T	S	G	I	I	M	G
Marmoset	C	A	T	S	G	I	I	M	G
Squirrel monkey	C	A	T	S	G	I	I	I	G
Bushbaby	C	A	T	S	G	I	I	M	G
Chinese tree shrew	C	A	S	S	G	I	I	M	G
Squirrel	C	A	T	S	G	I	V	M	G
Lesser Egyptian jerboa	C	A	T	S	G	I	I	M	G
Praire vole	C	A	T	S	G	I	I	M	G
Chinese hamster	C	A	T	S	G	I	I	M	G
Golden hamster	C	A	T	S	G	I	V	M	G
Mouse	C	A	T	S	G	I	I	M	G
Rat	C	A	T	S	G	I	I	M	G
Naked mole rat	C	A	A	S	G	I	A	L	G
Guniea pig	C	A	T	S	G	I	I	M	G
Chinchilla	C	A	T	S	G	I	I	M	G
Brush tailed rat	C	A	T	S	G	I	I	T	G
Rabbit	C	A	T	S	G	I	V	M	G
Pika	C	A	T	V	G	V	V	M	G
Pig	C	A	T	S	G	I	I	M	G
Alpaca	C	A	T	S	G	I	V	M	G
Bactrian camel	C	A	T	S	G	I	V	M	G
Dolphin	C	A	T	S	G	I	I	M	G
Killer whale	C	A	T	S	G	I	I	M	G
Tibetan antelope	C	A	T	S	G	I	I	M	G
Cow	C	A	T	S	G	I	I	M	G
Sheep	C	A	T	S	G	I	I	M	G
Domestic goat	C	A	T	S	G	I	I	V	G
Horse	C	A	T	S	G	I	I	M	G
White rhinoceros	C	A	T	S	G	I	I	M	G
Cat	C	A	T	S	G	I	I	M	G
Dog	C	A	T	S	G	I	I	M	G
Ferret	C	A	T	S	G	I	I	M	G
Panda	C	A	T	S	G	I	I	M	G
Pacific walrus	C	A	T	S	G	I	I	M	G
Weddell seal	C	A	T	S	G	I	I	M	G
Black flying fox	C	A	T	S	G	I	I	V	G
Megabat	C	A	T	S	G	I	I	V	G
David's myotis (bat)	C	A	T	S	G	I	I	M	G
Big brown bat	C	A	T	S	G	I	I	M	G
Hedgehog	C	A	T	S	G	I	I	M	G
Shrew	C	A	T	L	G	V	I	L	G
Star nosed mole	C	A	A	S	G	V	V	M	G
Elephant	C	A	T	S	G	I	I	L	G
Cape elephant shrew	C	A	T	S	G	I	I	L	G
Manatee	C	A	T	S	G	I	I	L	G
Cape golden mole	C	_	T	A	G	I	V	L	G
Tenrec	G	A	T	S	G	I	I	L	G
Aardvark	C	A	T	S	G	I	I	L	G

Fig 3. Identification of the pathogenic missense variation responsible for congenital cataracts in PKCC214. A) Individual 7 (unaffected; 35 yrs. old) heterozygous carrier and **B**) individual 11 (affected; 4 yrs. old), homozygous for the c.233G>A mutation. The variation results in a non-conservation substitution in MP19: p.G78D. Arrows point to the allele, c.233G, mutated in PKCC214. **C**) Sequence alignment of amino acids illustrating conservation of Gly78 among MP19 orthologs. Brown: Primates; green: Euarchontoglires; purple: Laurasiatheria; and orange: Afrotheria.

doi:10.1371/journal.pone.0162620.g003

expressed at lower levels at embryonic timepoints and expression increases considerably during early postnatal stages, remaining steady afterward. These data suggest a critical role for *LIM2* in the development of the ocular lens and the maintenance of its transparency.

Discussion

Here, we report a novel missense mutation in *LIM2* that segregates with autosomal recessive congenital cataracts in a consanguineous Pakistani family. Slit-lamp examination of the affected family members revealed nuclear cataracts. The medical records available to us indicate the cataracts developed during infancy. Linkage analysis determined the critical interval of 14.5 cM on chromosome 19, with a maximum LOD score of 3.25 at the recombination fraction of 0. Sequencing the *LIM2* gene identified a missense mutation, c.233G>A. This single-nucleotide variation resulted in a change from the nonpolar, smallest amino acid, glycine, to the larger, negatively charged aspartic acid. The glycine at position 78 is strongly conserved across different species. While the maximum LOD score of 3.25 is slightly higher than the traditional limiting value of 3.0, it represents the maximum value obtainable with this family. In addition,

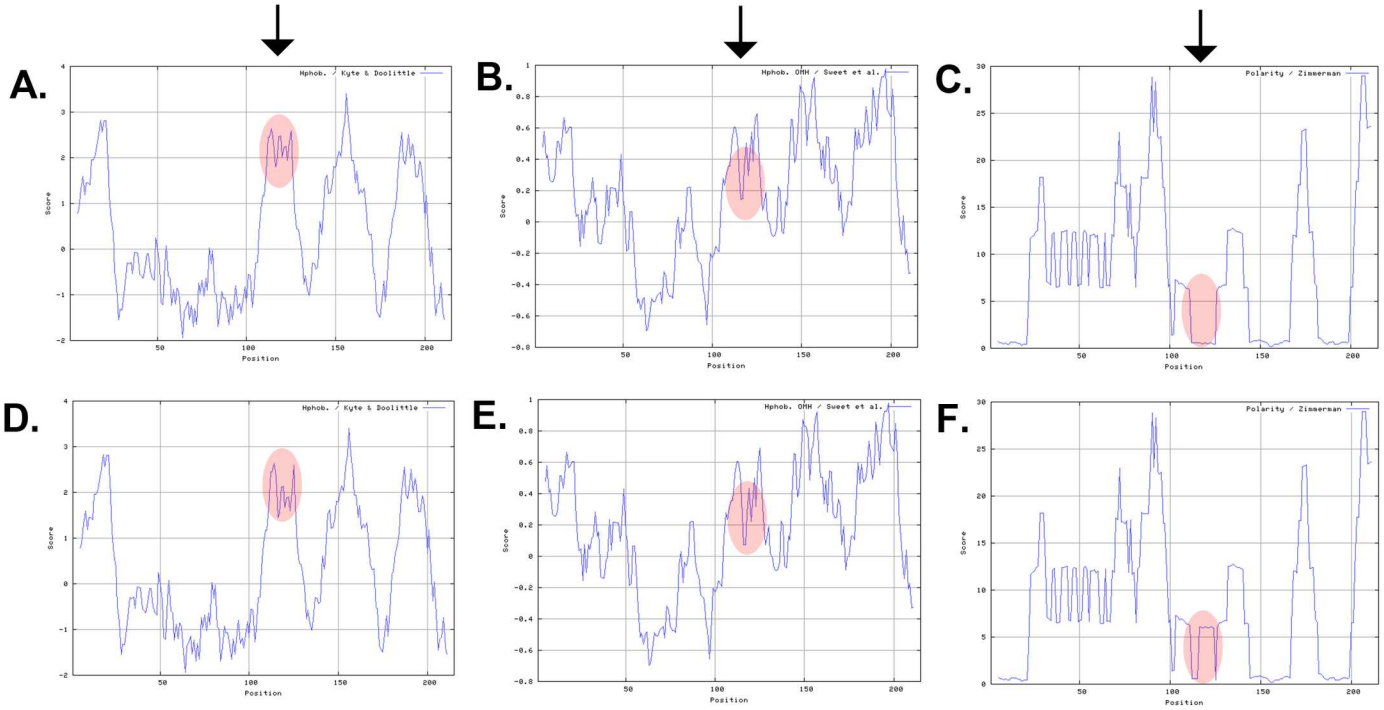

Fig 4. Investigating the physical characteristics of wild-type and mutant MP19. Mutant MP19 (p.G78D) exhibited lower hydropathicity (compare **A** with **D**), lower hydrophobicity (compare **B** with **E**), and higher polarity (compare **C** with **F**). The x-axis represents the position of the amino acids while the y-axis represents the hydropathicity, hydrophobicity, and polarity values in a default window size of 9. Arrows point to the difference in their respective hydropathicity (1st arrow), hydrophobicity (2nd arrow), and polarity (3rd arrow).

doi:10.1371/journal.pone.0162620.g004

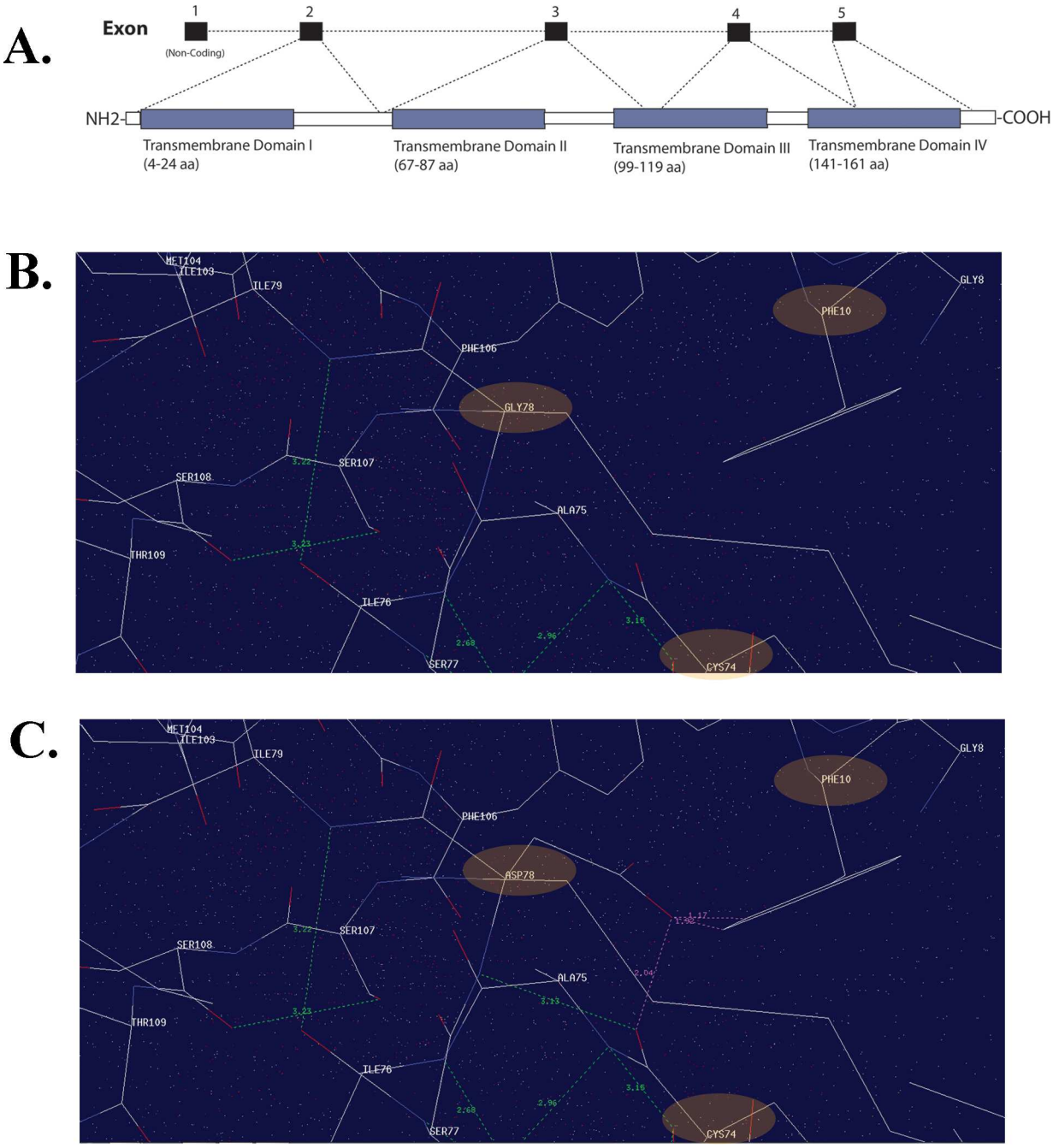

Fig 5. Missense mutation located in the transmembrane domain of MP19 is responsible for congenital cataracts. A) *LIM2* graphical illustration showing genomic architecture and MP19 protein structure, including the four transmembrane domains. Note: the topology has been obtained from Maher et al., 2012; Exp Eye Res.103:115–6. Molecular interactions of **B**) wild-type and **C**) mutant MP19 (harboring Gly78Asp) suggesting interactions of the mutant residue (D78) with the phenylalanine (F10) and cysteine (C74) residues.

doi:10.1371/journal.pone.0162620.g005

the lack of any LOD scores above 1.5 in the remainder of the genome-wide scan supports the localization of the cataract locus to chromosome 19q13.

Steel and colleagues reported the association of *LIM2* with lens opacity in To3 transgenic mice, identifying a single-base change in the first coding exon of *Lim2* that results in a glycine-

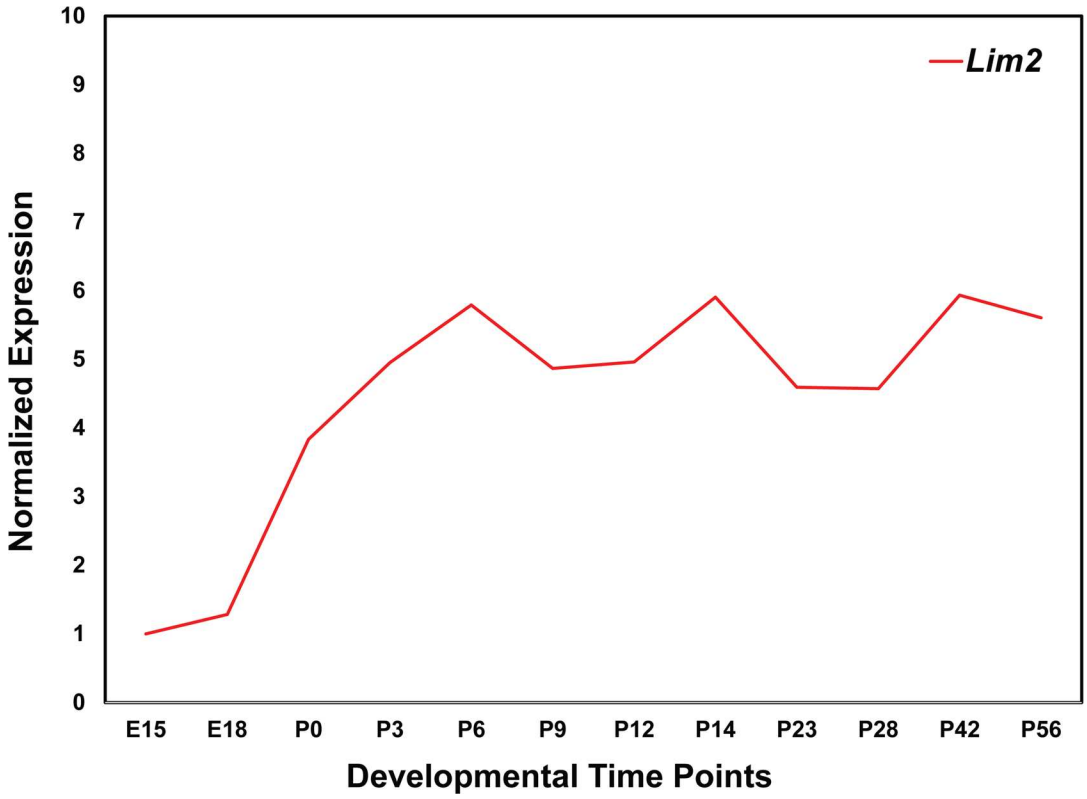

Fig 6. Expression profile of lens intrinsic membrane protein 2 (*Lim2*) in the developing mouse lens. The expression of *Lim2* at different developmental time points was normalized to *Gapdh*. The x-axis and y-axis represent developmental time points and normalized expression of *Lim2* mRNA, respectively.

doi:10.1371/journal.pone.0162620.g006

to-valine substituion at amino acid 15: c.44G>T (p.G15V) [38]. Chen and colleagues demonstrated that, in contrast to wild-type MP19 proteins, which localize to the cell membrane, mutant $MP19^{TO3}$ proteins are retained within subcellular compartments [39]. To understand the physiological significance of *LIM2* in lens morphogenesis, Shi and colleagues used both scanning electron and confocal microscopy to assess the contribution of *Lim2* to mouse lens tissue architecture, and concluded that Mp19 deficiency distinctly altered the characteristic morphology of mouse lens fiber cells. The researchers argued that their data suggested a critical role for Mp19 in the maintenance of cytoskeletal integrity, cell morphology, and intercellular communication in the mouse lens [40].

Previously, only two causal mutations in *LIM2* have been identified in patients with cataracts; the mutation identified here is now a third avenue of insight into the role of *LIM2* in cataractogenesis. Interestingly, the patients in each study exhibit different clinical characteristics than those of the other two studies, despite the cataracts being caused by mutations in the same gene. The patients reported by Pras and colleagues developed cataracts in their presenile years, which is in sharp contrast to members of PKCC214 and the patients reported by Ponnam and colleagues, who all exhibited cataractogenesis with early onset (Table 4). Moreover, the patients of Pras et al. exhibited no additional ocular anomalies, while cataract development in PKCC214 and the patients reported by Ponnam et al. was concurrent with nystagmus (Table 4). Last but not least, the cataracts themselves are morphologically different in all three reports. The patients in the family reported by Pras et al. exhibited cortical bluish and white opacifications in concentric layers, with nuclear opacities emerging from prominent sutures

Table 4. Summary of mutations identified in *LIM2* associated with cataractogenesis.

No	Nucleotide Change	Amino Acid Change	Exon	Cataractogenesis Onset	Cataract Phenotype	Additional Phenotypes	Ethnicity	Reference
1	c.313T>G	p.F105V	3	Presenile	pulverulent cortical/ nuclear	-	Iraqi/ Arab	[17]
2	c.587G>A	p.G154E	4/5	Congenital	total	nystagmus; dense amblyopia	Indian	[31]
3	c.233G>A	p.G78D	3	Congenital	nuclear	nystagmus	Pakistani	current study

doi:10.1371/journal.pone.0162620.t004

(Table 4). In contrast, patients reported by Ponnam et al. had total cataracts while members of PKCC214 manifested nuclear cataracts (Tables 2 & 4).

The mechanism of cataractogenesis remains elusive, including the particular effects of missense mutations in *LIM2*. It is notable that all three mutations affect conserved amino acids, and that each missense change has an autosomal recessive loss of function mode of inheritance. Interestingly, all three mutated amino acids reside in transmembrane domains of MP19, according to the topology reported by Maher and colleagues [41]. The missense changes reported by Pras et al. and Ponnam et al. [c.313T>G (p.F105V) and c.587G>A (p.G154E)] reside in the third and fourth transmembrane domains of MP19, while the missense change in PKCC214 [c.233G>A (p.G78D)] is predicted to reside in the second transmembrane domain. Given that all of the missense changes are responsible for cataractogenesis, it is tempting to speculate that the altered topology of MP19 (a likely result of missense mutations compromising conserved regions) affects translocation to the cell membrane or the protein's physiological function at the membrane. Nonetheless, detailed mechanistic analysis of these mutant proteins, especially their relationships to one another, will contribute significantly in discovering the pathomechanism of cataractogenesis.

In conclusion, we report a missense mutation in the sequence of *LIM2* encoding the second transmembrane domain of MP19 that causes autosomal recessive congenital cataracts. Identification of the genetic origins of cataractogenesis will help us to better understand the biology of the ocular lens, including mechanistic details of the maintenance of lens transparency.

Supporting Information

S1 File. The ARRIVE checklist has been completed for the manuscript.
(PDF)

Acknowledgments

The authors are grateful to all those who gave their time and effort to participate in this study.

Author Contributions

Conceptualization: BI SYK MAN SNK SR SAR.

Formal analysis: BI SYK MA HK FK BR FF RN AOK SAO MAN IAN SNK TH SR JA AOE SAR.

Funding acquisition: AOK SAO SNK TH SR JA SAR.

Investigation: BI SYK MA HK FK BR.

Project administration: SNK TH SR JA SAR.

Resources: AOK SAO SNK TH SR SAR.

Supervision: SNK TH SR JA SAR.

Validation: SNK TH SR JA SAR.

Writing – original draft: BI SYK FK BR AOK SAO SR SAR.

Writing – review & editing: BI SYK FK BR AOK SAO SR SAR.

References

1. Robinson GC, Jan JE, Kinnis C (1987) Congenital ocular blindness in children, 1945 to 1984 1502. Am J Dis Child 141: 1321–1324. PMID: 3687875
2. Shiels A, Hejtmancik JF (2007) Genetic origins of cataract. Arch Ophthalmol 125: 165–173. 125/2/165 [pii]; doi: 10.1001/archopht.125.2.165 PMID: 17296892
3. Merin S, Crawford JS (1971) The etiology of congenital cataracts. A survey of 386 cases. Can J Ophthalmol 6: 178–182. PMID: 4254831
4. Butt T, Yao W, Kaul H, Xiaodong J, Gradstein L, Zhang Y et al. (2007) Localization of autosomal recessive congenital cataracts in consanguineous Pakistani families to a new locus on chromosome 1p. Mol Vis 13: 1635–1640. PMID: 17893665
5. Kaul H, Riazuddin SA, Shahid M, Kousar S, Butt NH, Zafar AU et al. (2010) Autosomal recessive congenital cataract linked to EPHA2 in a consanguineous Pakistani family. Mol Vis 16: 511–517. PMID: 20361013
6. Ponnam SP, Ramesha K, Tejwani S, Ramamurthy B, Kannabiran C (2007) Mutation of the gap junction protein alpha 8 (GJA8) gene causes autosomal recessive cataract. J Med Genet 44: e85. doi: 10.1136/jmg.2007.050138 PMID: 17601931
7. Pras E, Pras E, Bakhan T, Levy-Nissenbaum E, Lahat H, Assia EI et al. (2001) A gene causing autosomal recessive cataract maps to the short arm of chromosome 3. Isr Med Assoc J 3: 559–562. PMID: 11519376
8. Sabir N, Riazuddin SA, Butt T, Iqbal F, Nasir IA, Zafar AU et al. (2010) Mapping of a new locus associated with autosomal recessive congenital cataract to chromosome 3q. Mol Vis 16: 2634–2638. PMID: 21179239
9. Pras E, Raz J, Yahalom V, Frydman M, Garzozi HJ, Pras E et al. (2004) A nonsense mutation in the glucosaminyl (N-acetyl) transferase 2 gene (GCNT2): association with autosomal recessive congenital cataracts. Invest Ophthalmol Vis Sci 45: 1940–1945. PMID: 15161861
10. Kaul H, Riazuddin SA, Yasmeen A, Mohsin S, Khan M, Nasir IA et al. (2010) A new locus for autosomal recessive congenital cataract identified in a Pakistani family. Mol Vis 16: 240–245. PMID: 20161816
11. Sabir N, Riazuddin SA, Kaul H, Iqbal F, Nasir IA, Zafar AU et al. (2010) Mapping of a novel locus associated with autosomal recessive congenital cataract to chromosome 8p. Mol Vis 16: 2911–2915. PMID: 21203409
12. Heon E, Paterson AD, Fraser M, Billingsley G, Priston M, Balmer A et al. (2001) A progressive autosomal recessive cataract locus maps to chromosome 9q13-q22. Am J Hum Genet 68: 772–777. doi: 10.1086/318798 PMID: 11179024
13. Safieh LA, Khan AO, Alkuraya FS (2009) Identification of a novel CRYAB mutation associated with autosomal recessive juvenile cataract in a Saudi family. Mol Vis 15: 980–984. 103 [pii]. PMID: 19461931
14. Smaoui N, Beltaief O, BenHamed S, M'Rad R, Maazoul F, Ouertani A et al. (2004) A homozygous splice mutation in the HSF4 gene is associated with an autosomal recessive congenital cataract. Invest Ophthalmol Vis Sci 45: 2716–2721. doi: 10.1167/iovs.03-1370 PMID: 15277496
15. Yasmeen A, Riazuddin SA, Kaul H, Mohsin S, Khan M, Qazi ZA et al. (2010) Autosomal recessive congenital cataract in consanguineous Pakistani families is associated with mutations in GALK1. Mol Vis 16: 682–688. PMID: 20405025
16. Riazuddin SA, Yasmeen A, Zhang Q, Yao W, Sabar MF, Ahmed Z et al. (2005) A new locus for autosomal recessive nuclear cataract mapped to chromosome 19q13 in a Pakistani family. Invest Ophthalmol Vis Sci 46: 623–626. doi: 10.1167/iovs.04-0955 PMID: 15671291
17. Pras E, Levy-Nissenbaum E, Bakhan T, Lahat H, Assia E, Geffen-Carmi N et al. (2002) A missense mutation in the LIM2 gene is associated with autosomal recessive presenile cataract in an inbred Iraqi Jewish family. Am J Hum Genet 70: 1363–1367. doi: 10.1086/340318 PMID: 11917274

18. Ramachandran RD, Perumalsamy V, Hejtmancik JF (2007) Autosomal recessive juvenile onset cataract associated with mutation in BFSP1. Hum Genet 121: 475–482. doi: 10.1007/s00439-006-0319-6 PMID: 17225135

19. Pras E, Frydman M, Levy-Nissenbaum E, Bakhan T, Raz J, Assia EI et al. (2000) A nonsense mutation (W9X) in CRYAA causes autosomal recessive cataract in an inbred Jewish Persian family. Invest Ophthalmol Vis Sci 41: 3511–3515. PMID: 11006246

20. Riazuddin SA, Yasmeen A, Yao W, Sergeev YV, Zhang Q, Zulfiqar F et al. (2005) Mutations in betaB3-crystallin associated with autosomal recessive cataract in two Pakistani families. Invest Ophthalmol Vis Sci 46: 2100–2106. doi: 10.1167/iovs.04-1481 PMID: 15914629

21. Chen J, Ma Z, Jiao X, Fariss R, Kantorow WL, Kantorow M et al. (2011) Mutations in FYCO1 cause autosomal-recessive congenital cataracts. Am J Hum Genet 88: 827–838. S0002-9297(11)00201-1 [pii]; doi: 10.1016/j.ajhg.2011.05.008 PMID: 21636066

22. Aldahmesh MA, Khan AO, Mohamed JY, Alghamdi MH, Alkuraya FS (2012) Identification of a truncation mutation of acylglycerol kinase (AGK) gene in a novel autosomal recessive cataract locus. Hum Mutat 33: 960–962. doi: 10.1002/humu.22071 PMID: 22415731

23. Lachke SA, Alkuraya FS, Kneeland SC, Ohn T, Aboukhalil A, Howell GR et al. (2011) Mutations in the RNA granule component TDRD7 cause cataract and glaucoma. Science 331: 1571–1576. 331/6024/1571 [pii]; doi: 10.1126/science.1195970 PMID: 21436445

24. Zhao L, Chen XJ, Zhu J, Xi YB, Yang X, Hu LD et al. (2015) Lanosterol reverses protein aggregation in cataracts. Nature 523: 607–611. nature14650 [pii]; doi: 10.1038/nature14650 PMID: 26200341

25. Cohen D, Bar-Yosef U, Levy J, Gradstein L, Belfair N, Ofir R et al. (2007) Homozygous CRYBB1 deletion mutation underlies autosomal recessive congenital cataract. Invest Ophthalmol Vis Sci 48: 2208–2213. doi: 10.1167/iovs.06-1019 PMID: 17460281

26. Arneson ML, Louis CF (1998) Structural arrangement of lens fiber cell plasma membrane protein MP20. Exp Eye Res 66: 495–509. doi: 10.1006/exer.1998.0477 PMID: 9593642

27. Gutekunst KA, Rao GN, Church RL (1990) Molecular cloning and complete nucleotide sequence of the cDNA encoding a bovine lens intrinsic membrane protein (MP19). Curr Eye Res 9: 955–961. PMID: 2276272

28. Mulders JW, Voorter CE, Lamers C, de Haard-Hoekman WA, Montecucco C, van d V et al. (1988) MP17, a fiber-specific intrinsic membrane protein from mammalian eye lens. Curr Eye Res 7: 207–219. PMID: 3371069

29. Louis CF, Hur KC, Galvan AC, TenBroek EM, Jarvis LJ, Eccleston ED et al. (1989) Identification of an 18,000-dalton protein in mammalian lens fiber cell membranes. J Biol Chem 264: 19967–19973. PMID: 2584203

30. TenBroek E, Arneson M, Jarvis L, Louis C (1992) The distribution of the fiber cell intrinsic membrane proteins MP20 and connexin46 in the bovine lens. J Cell Sci 103 (Pt 1): 245–257.

31. Ponnam SP, Ramesha K, Tejwani S, Matalia J, Kannabiran C (2008) A missense mutation in LIM2 causes autosomal recessive congenital cataract. Mol Vis 14: 1204–1208. PMID: 18596884

32. Jiaox X, Khan SY, Irum B, Khan AO, Wang Q, Kabir F et al. (2015) Missense Mutations in CRYAB Are Liable for Recessive Congenital Cataracts. PLoS One 10: e0137973. doi: 10.1371/journal.pone.0137973 PONE-D-15-12822 [pii]. PMID: 26402864

33. Jiao X, Kabir F, Irum B, Khan AO, Wang Q, Li D et al. (2016) A Common Ancestral Mutation in CRYBB3 Identified in Multiple Consanguineous Families with Congenital Cataracts. PLoS One 11: e0157005. doi: 10.1371/journal.pone.0157005 PONE-D-15-23789 [pii]. PMID: 27326458

34. Lathrop GM, Lalouel JM (1984) Easy calculations of lod scores and genetic risks on small computers. Am J Hum Genet 36: 460–465. PMID: 6585139

35. Schaffer AA, Gupta SK, Shriram K, Cottingham RW (1994) Avoiding recomputation in genetic linkage analysis. Hum Hered 44: 225–237. PMID: 8056435

36. Zhou L, Li X, Church RL (2001) The mouse lens fiber-cell intrinsic membrane protein MP19 gene (Lim2) and granule membrane protein GMP-17 gene (Nkg7): Isolation and sequence analysis of two neighboring genes. Mol Vis 7: 79–88. v7/a12 [pii]. PMID: 11290961

37. Khan SY, Hackett SF, Lee MC, Pourmand N, Talbot CC Jr., Riazuddin SA (2015) Transcriptome Profiling of Developing Murine Lens Through RNA Sequencing. Invest Ophthalmol Vis Sci 56: 4919–4926. 2422128 [pii]; doi: 10.1167/iovs.14-16253 PMID: 26225632

38. Steele EC Jr., Kerscher S, Lyon MF, Glenister PH, Favor J, Wang J et al. (1997) Identification of a mutation in the MP19 gene, Lim2, in the cataractous mouse mutant To3. Mol Vis 3: 5. PMID: 9238094

39. Chen T, Li X, Yang Y, Church RL (2002) Localization of lens intrinsic membrane protein MP19 and mutant protein MP19(To3) using fluorescent expression vectors. Mol Vis 8: 372–388. v8/a45 [pii]. PMID: 12379840

40. Shi Y, De Maria AB, Wang H, Mathias RT, FitzGerald PG, Bassnett S (2011) Further analysis of the lens phenotype in Lim2-deficient mice. Invest Ophthalmol Vis Sci 52: 7332–7339. iovs.11-7724 [pii]; doi: 10.1167/iovs.11-7724 PMID: 21775657

41. Maher GJ, Black GC, Manson FD (2012) Focus on molecules: lens intrinsic membrane protein (LIM2/MP20). Exp Eye Res 103: 115–116. S0014-4835(11)00236-3 [pii]; doi: 10.1016/j.exer.2011.08.006 PMID: 21867698